Soil Dynamics and Earthquake Engineering 65 (2014) 142–150

Contents lists available at ScienceDirect

Soil Dynamics and Earthquake Engineering

journal homepage: www.elsevier.com/locate/soildyn

# Effect of non-plastic silt content on the liquefaction behavior of sand–silt mixture

Mohammad Emdadul Karim, Md. Jahangir Alam *

*Department of Civil Engineering, Bangladesh University of Engineering and Technology (BUET), Dhaka 1000, Bangladesh*

ARTICLE INFO

*Article history:*
Received 13 March 2013
Received in revised form
28 September 2013
Accepted 8 June 2014

*Keywords:*
Liquefaction
Limiting silt content
Cyclic shear strength
Excess pore pressure

ABSTRACT

To identify the effect of non-plastic silt on the cyclic behavior of sand–silt mixtures, total sixty undrained cyclic triaxial stress-control tests were carried out on sand–silt mixtures. These tests were conducted on specimens of size 71 mm diameter and 142 mm height with a frequency of 1 Hz. Specimens were prepared at a constant relative density and constant density approach. The effect of relative density, confining pressure as well as magnitude of cyclic loading was also studied. For a constant relative density ($D_r$=60%) the effect of limiting silt content, pore pressure response and cyclic strength was observed. The rate of generation of excess pore water pressure with respect to cycles of loading was found to initially increase with increase in silt content till the limiting silt content and thereafter it reverses its trend when the specimens were tested at a constant relative density. The cyclic resistance behavior was observed to be just opposite to the pore pressure response. Permeability, CRR and secant shear modulus decreased till limiting silt content; after that they became constant with increasing silt content.



## 1. Introduction

A soil may or may not liquefy, but the amount of excess pore water pressure generated during static or cyclic loading considerably affects its strength and stiffness. Generation of excess pore water pressure and subsequent liquefaction of saturated sandy soils with or without fines has been a topic of extensive laboratory research since the last 50 years. Most of the earlier research was focused on clean sands with an idea that the presence of fines in a sand deposit resists the development of pore water pressure. However, large-scale liquefaction related failures in silty sand deposits in earthquakes of recent past changed this idea and most of the present researches are more focused on the influence of fines in controlling the pore pressure response and hence the liquefaction behavior of sandy soils. The pore pressure generation is dependent on the deformational characteristics of silty sands and sandy silts, which is quite different from that of clean sand.

Study on liquefaction of sands started greatly after the Niigata Earthquake of 1964 and the Alaska Earthquake of 1964 which caused dramatic damages due to liquefaction. Most of the earlier research was focused on clean sands with an idea that the presence of fines in a sand deposit resists the development of pore water pressure. However, Kishida [1] reported liquefaction of soils with up to 70% fines and 10% clay fraction during Mino-Owar, Tohankai and Fukui earthquakes. Tohno and Yasuda [2] reported that soils with fines up to 90% and clay content of 18% exhibited liquefaction during the Tokachi–Oki earthquake of 1968. Soils with up to 48% fines and 18% clay content were found to have liquefied during the Hokkaido Nansai–Oki earthquake of 1993. Seed et al. [3] have recommended that for sands containing less than 5% fines, the effect of fines may be neglected. For sands containing more than 5% fines, the liquefaction potential decreases.

Increase [4,5], decrease [6,7] and initial decrease till limiting silt content and thereafter an increase [8–12] in cyclic resistance with increase in silt content at a constant gross void ratio has been reported in Fig. 1 [13]. At a constant relative density, Singh [14] reported a decrease whereas Polito and Martin II [8] reported an initial constant cyclic resistance till limiting silt content, followed by a drastic fall till a relatively stable level, but Dash and Sitharam [15] reported an initial increase of cyclic resistance till around 5% silt content and then a drastic decrease till the limiting silt content and thereafter a more or less same rate till even pure silt. Similarly at a constant sand skeleton void ratio, increase in cyclic resistance with increase in fines content was reported by Shen et al. [16], Kuerbis et al. [17], Vaid [18] and Xenaki and Athanasopoulos [10], whereas Finn et al. [7] and Polito and Martin [8] reported a constant behavior. Lee and Albaisa [19] and Dash and Sitharam [15] also suggested pore pressure band by examining the pore pressure response against the cycle ratio (i.e. the ratio of cycles of loading to the cycles of loading required for initial liquefaction).

* Corresponding author.
*E-mail addresses:* emdadul.buet@gmail.com (M.E. Karim), jahangir.buet@gmail.com (Md.J. Alam).

http://dx.doi.org/10.1016/j.soildyn.2014.06.010
0267-7261/

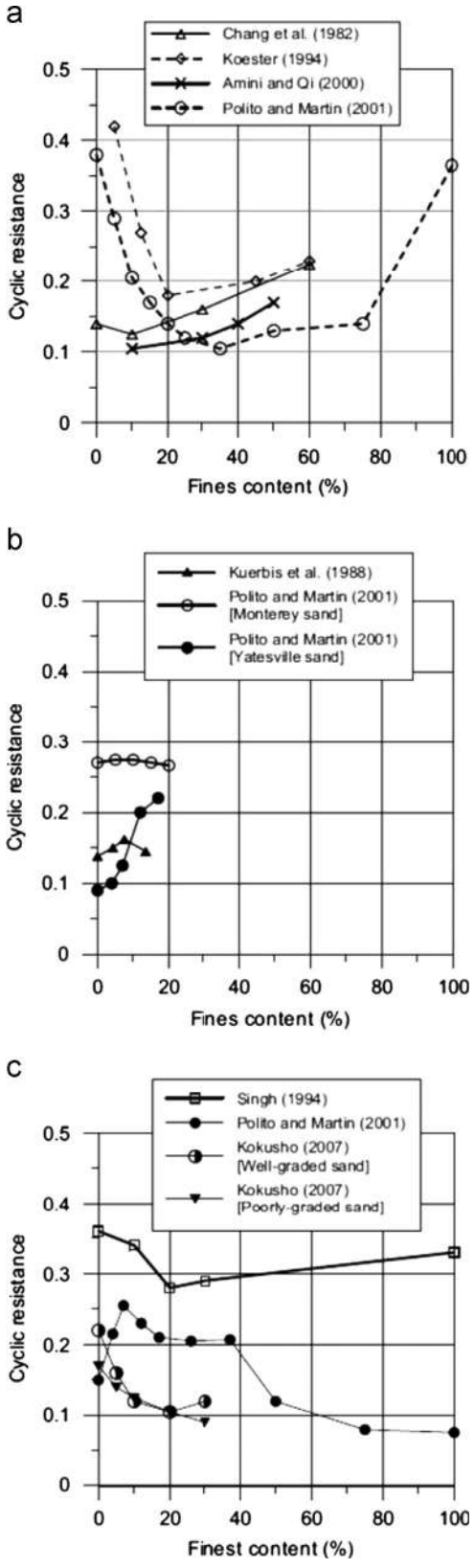


**Fig. 1.** Results from previous studies on the effect of fines content (FC) on cyclic resistance: (a) studies at constant overall void ratio; (b) studies at constant sand skeleton void ratio; and (c) studies at constant relative density.

The curves obtained by plotting excess pore pressure ratio against cycle ratio fell within a relatively narrow band for a wide range of relative densities and consolidation pressures.

In view of these conflicting conclusions even at a particular measure of density, a detailed laboratory investigation program through stress controlled cyclic triaxial tests was carried out to study and clarify the effects of non-plastic fines and other parameters on the undrained pore water pressure response of sand and silt mixtures. The effect of non-plastic fines was studied by preparing specimens to various measures of density through the constant dry density approach and the constant relative density approach. The effect of relative density, confining pressure as well as the magnitude of cyclic loading was also studied. Falling head permeability test was conducted on sand–silt mixtures to explain the effect of fines content on liquefaction behavior.

## 2. Experimental program

### 2.1. Materials used

Fine sand and silt were collected from sandbars of Padma River, Mawa, Munshiganj, Bangladesh, near the proposed Padma Bridge site. Fine sand and silt both were oven dried and then sieved through a 75 μm sieve to obtain the clean sand and silt. The grain size distributions of clean sand, silt and sand–silt mixtures are presented in Fig. 2. Plastic limit of silt was determined and it was observed that the silt was non-plastic. Index properties of sand and silt are shown in Table 1. Fine sand and silt specimen were viewed under a scanning electron microscope (SEM) to see the shape of particles. Photo 1 shows the image of fine sand with 50 times magnification and Photo 2 shows the image of silt with 150 times magnification. From these two images from SEM it is clearly seen that the fine sand and silt particles are angular and rough. This means both fine sand and silt have the same granular material with different particle sizes. Hence, non-plastic silt does not show plasticity behavior.

To estimate mica content in the fine sand and nonplastic silt, stereo optical microscope was used to count the percent of mica particles in a selected small amount of sand and silt. It is found that mica exists about 1% in sand and 3% in silt. This percent is based on particle count, not based on weight or volume.

Sand–silt mixtures were prepared by adding non-plastic silt in various percentages (by weight of total soil) to the clean sand. Maximum and minimum index densities of sand–silt mixtures are determined and shown in Table 2 and Fig. 3(a). Maximum and minimum void ratios of sand–silt mixtures are shown in Fig. 3(b). Maximum density was determined by the modified proctor test and minimum density was determined by minimum density test in water method [21]. Cyclic triaxial tests were performed on sand–silt mixtures with various cyclic stress ratios. The experimental program is shown in Table 3.

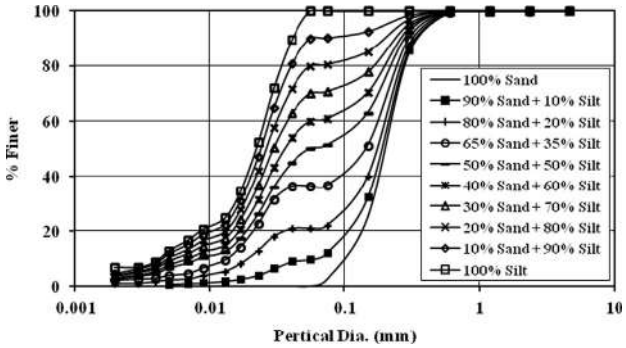


**Fig. 2.** Grain size distribution of clean sand, non-plastic silt and sand–silt mixtures used in this study.

**Table 1**
Index properties of component soils used in this study.

| Soil type | Sand | Silt |
|---|---|---|
| USCS classification | Poorly graded sand | Silt |
| Mean grain size $D_{50}$ (mm) | 0.203 | 0.022 |
| Uniformity coefficient ($C_u$) | 2.18 | 5.233 |
| Coefficient of gradation ($C_z$) | 1.13 | 2.191 |
| Specific gravity ($G_s$) | 2.69 | 2.72 |
| Minimum index density (kN/m$^3$) | 12.17 | 9.81 |
| Maximum index density (kN/m$^3$) | 17.544 | 18.259 |
| Minimum index void ratio ($e_{min}$) | 0.504 | 0.462 |
| Maximum index void ratio ($e_{max}$) | 1.165 | 1.72 |
| Liquid limit (%) | NP[a] | NP[a] |
| Plastic limit (%) | ND[b] | ND[b] |
| Plasticity Index (%) | NP[a] | NP[a] |

[a] NP=non-plastic.
[b] ND=not determinable.

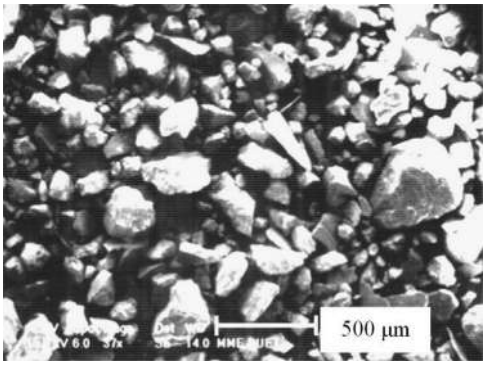


**Photo 1.** Image of fine sand at 37 times magnification in scanning electron microscope (SEM).

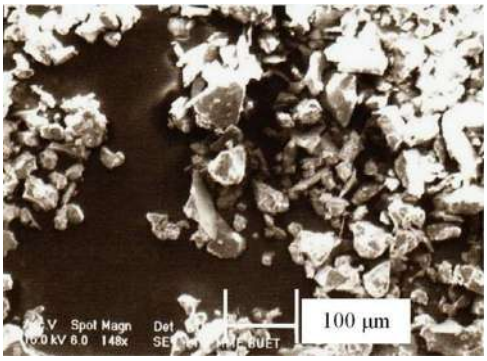


**Photo 2.** Image of silt at 148 times magnification in scanning electron microscope (SEM).

**Table 2**
Minimum and maximum index density of various sand–silt mixtures used in this study.

| Soil types | Maximum density | Minimum density |
|---|---|---|
| 100% sand | 17.508 | 12.167 |
| 90% sand+10% silt | 18.100 | 11.753 |
| 80% sand+20% silt | 18.361 | 11.546 |
| 70% sand+30% silt | 18.800 | 11.200 |
| 60% sand+35% silt | 18.928 | 11.027 |
| 50% sand+50% silt | 19.446 | 11.178 |
| 40% sand+60% silt | 18.930 | 10.553 |
| 30% sand+70% silt | 19.000 | 10.441 |
| 20% sand+80% silt | 18.276 | 9.964 |
| 10% sand+90% silt | 18.389 | 9.913 |
| 100% silt | 18.259 | 9.814 |

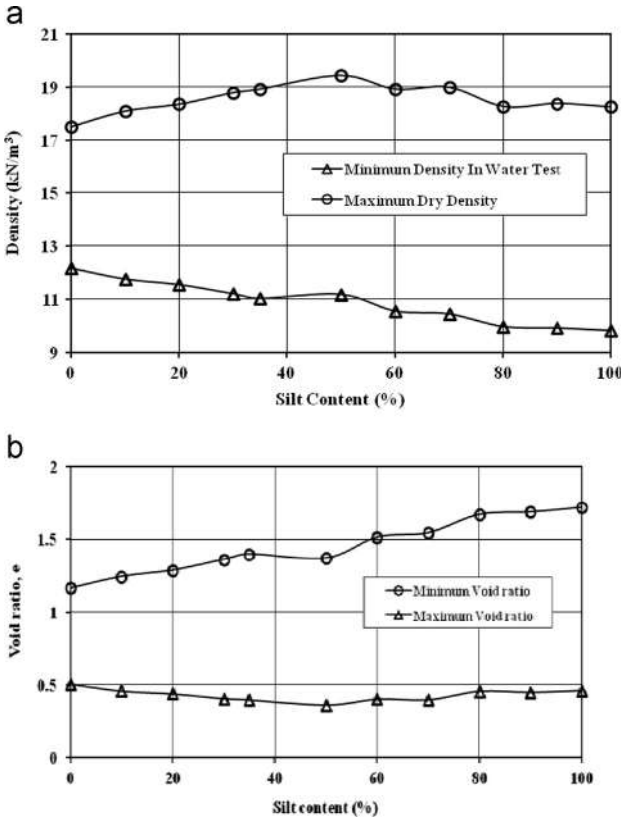


**Fig. 3.** (a) Maximum and minimum density versus percent of silt content and (b) minimum and maximum void ratio versus percent of silt content.

**Table 3**
Experimental program of cyclic triaxial test.

| Soil types | $\sigma_{3c'}$ (kPa) | Frequency $f$ (Hz) | CSR | Relative density (%), $D_r$ |
|---|---|---|---|---|
| 100% sand | 50, 100 | 1 | 0.08–0.20 | 32, 38, 60 |
| 90% sand+10% silt | 100 | 1 | 0.08–0.20 | 60 |
| 80% sand+20% silt | 100 | 1 | 0.08–0.20 | 60 |
| 70% sand+30% silt | 100 | 1 | 0.08–0.20 | 32, 60 |
| 60% sand+35% silt | 100 | 1 | 0.08–0.20 | 60 |
| 50% sand+50% silt | 100 | 1 | 0.08–0.20 | 40, 60 |
| 40% sand+60% silt | 100 | 1 | 0.08–0.20 | 60 |
| 30% sand+70% silt | 100 | 1 | 0.08–0.20 | 60 |
| 20% sand+80% silt | 100 | 1 | 0.08–0.20 | 60 |
| 10% sand+90% silt | 100 | 1 | 0.08–0.20 | 60 |
| 100% silt | 100 | 1 | 0.08–0.20 | 60 |

### 2.2. Limiting fines content

Limiting fines content (LFC) was first thoroughly investigated by Polito [20]. Later Hazirbaba [22] proposed an equation to estimate LFC. As fines (silt) are added to a sand, it passes from one phase to the other through a transition point called the limiting fines (silt) content. Below this point the soil structure is generally a sand-dominated one with silt contained in a sand-skeleton whereas beyond this point there are enough fines such that the sand grains loose contact with each other and the soil structure becomes predominantly a silt-dominated one. LFC is calculated using the following expression [21]:

$$\mathrm{LFC} = \frac{W_{\mathrm{fines}}}{W_{\mathrm{sand}} + W_{\mathrm{fines}}} = \frac{G_f e_s}{G_f e_s + G_s(1+e_f)} \quad (1)$$

where $W_{\mathrm{fines}}$ is the weight of fines and $W_{\mathrm{sand}}$ is the weight of sand in a sand–silt mixture. Similarly, $G_f$, $G_s$, $e_f$ and $e_s$ stand for specific

gravity of fines, specific gravity of sand, maximum index void ratio of fines and maximum index void ratio of sand, respectively. Using Eq. (1), the limiting silt content for sand–silt mixtures used in this study was found to be 30%.

In Fig. 4(a) and (b), where the inner void decreases with increasing the fines content, the fine particles fill the inner void spaces between the large grains until point (b) is reached (LFC phase). At this point the inner void spaces are almost completely filled by the fines. From point (b) the large particles start to separate from each other, from where the silt-dominant part starts. Between points (b) and (c) the large particles become significantly displaced from each other by the large quantity of smaller particles until it reaches (d). From the LFC phase the inner void of the fines becomes equal. So it behaves similar to silt.

### 2.3. Specimen preparation

Soil specimens used in this study were 71 mm in diameter and 142 mm in height. The specimens were formed using wet tamping method in a split mold. The inner diameter of the mold is 71 mm and height 142 mm. The dry soil is mixed with 10% water and then compacted in several equal layers by a hammer that delivers some blows to each layer to achieve the target relative density. Number of layers and number of blows per layer were determined by trial to achieve the target relative density. The hammer weighs 1 kg, and has a drop of 6 in. In order to obtain a uniform density throughout the specimen, the compaction method of specimen preparation suggested by Ladd [23] was used.

### 2.4. Saturation and consolidation

Once the preparation of the specimen was complete and the specimen was formed, initial saturation of the specimen was done by passing carbon dioxide about one hour through the specimen. After that the distilled water was passed through the specimen by a gravity pressure of 5 kPa for 3–5 h. At the end of this process the cyclic machine was switched on. The machine is capable of applying sufficient back pressure till it was ensured that Skempton's $B$ parameter is equal to 95%. The specimens were then isotropically consolidated to a desired effective confining stress. The duration for the process of consolidation was varied from about 2 h (for clean sands) to about 3 h (for pure silt). All relative densities reported here are post-consolidation relative densities. After consolidation cyclic load was applied at various cyclic stress ratios.

### 2.5. Cyclic triaxial testing equipment

The testing apparatus used in the current study is capable of conducting static as well as cyclic tests. The triaxial system consists of the following components: triaxial cell, loading frame with computer-controlled platen that applies axial load on top of soil specimen, two computer-controlled flow pumps to control the chamber pressure and back pressure, high performance linear servo control electro actuator for cyclic loading with update rates of 500 times per second, micro-processor for controlling cyclic loading, a computer to control the test and a data logger. Various transducers are mounted in the system for measuring the axial load, confining pressure, pore-water pressure and axial strain. All tests were conducted at a cyclic loading frequency of 1 Hz, because for the time being the apparatus only can operate in 1 Hz. The excess pore water pressures were measured at the bottom of each specimen. Before starting the cyclic deviator load the triaxial cell was needed to make quarter inch empty which is filled with pressurized air cushion at the same cell pressure. The specimens were then loaded with a sinusoidal deviator stress at the appropriate cyclic stress ratio (CSR) until they liquefied.

## 3. Test result and discussion

### 3.1. Typical test result

The results of a typical cyclic triaxial test, performed on a specimen with 20% silt content prepared to a post-consolidation relative density 60% and loaded at a cyclic stress ratio of 0.10, are presented in Fig. 5. The constant load applied to the specimen till $\pm 3\%$ axial strain was developed as shown in Fig. 5(a). The employed actuator is a pneumatic device that is operated by air pressure. This is the reason why the cyclic load of 1 Hz frequency in Fig. 5 could not achieve the prescribed amplitude when strain exceeded 3%. Use of lower frequency may solve the problem.

The corresponding axial strain induced on the specimen is presented in Fig. 5(b) against the cycles of loading. It is to be noted here that the specimen achieved nearly 100% excess pore water pressure at the 9th cycle of uniform loading in the test for which Fig. 5 is presented. The pore water pressures generated in the specimen as a result of the induced axial strains are presented in Fig. 5(c). It may be seen in these figures that the deviator stress remained unaltered till the end of the test. The axial strain development on the specimen remained very low at initial cycles of loading but it drastically increased towards the end. This drastic increase in axial strain started corresponding to around 80% excess pore water pressure generation. At this point stress state may have touched the failure envelope. The effective stress path of the specimen is presented in Fig. 5(d) where the shear stress $\tau = (\sigma'_1 - \sigma'_3)/2$ and normal stress $\sigma' = (\sigma'_1 + \sigma'_3)/2$, where it can be seen that the specimen loses all its strength and stiffness corresponding to nearly 100% excess pore water pressure generation. Similar observation was made in all other tests. To identify the effective failure stress line, one strain-controlled static triaxial test was carried out at the same relative density of 60% on the specimen with 20% silt content. The angle of effective failure stress line is found to be 27°, which is shown in Fig. 5(d).

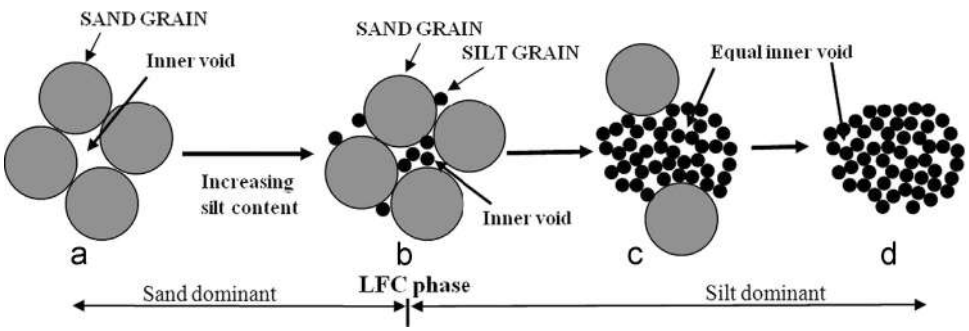


**Fig. 4.** Schematic diagram demonstrating particle arrangement of sand–silt mixture with the variation of silt content.

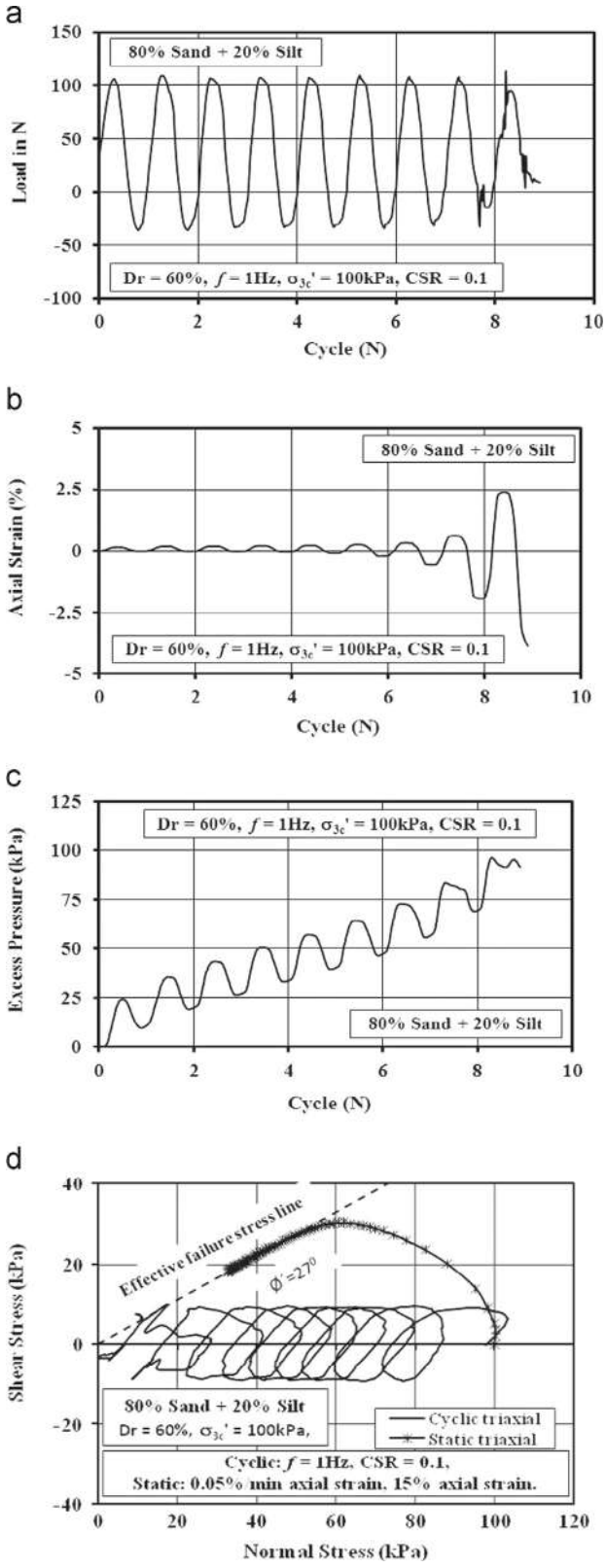


**Fig. 5.** (a) Deviator stress versus cycles of loading till ±3% axial strain; (b) axial strain versus cycles of loading till ±3% axial strain; (c) pore water pressure response till ±3% axial strain; and (d) effective stress path.

Again, a typical pore pressure response analysis is presented in Fig. 6. The pore pressure response in the specimens prepared to a constant post-consolidation relative density of 60% is presented in this figure as per the method suggested by Lee and Albaisa [19]; Dash and Sitharam [15]. The peak excess pore water pressure ratio corresponding to various cycles of loading has been plotted in this figure against the cycle ratio. Excess pore water ratio ($R_u$) is defined as the ratio of excess pore water pressure ($u_{excess}$) generated during a particular cycle of loading to the initial effective confining pressure ($\sigma'_{3c}$). Similarly the peak pore pressure ratio is the maximum pore water pressure ratio at a particular cycle of loading. The cycle ratio ($N/N_L$) is defined as the ratio of cycle of loading ($N$) to the cycles of loading till 100% excess pore water pressure (i.e. the point of initial liquefaction) or ±3% axial strain is generated ($N_L$). It can be seen in Fig. 6 that the peak pore pressures in sand–silt mixtures deviate the upper and lower bound values suggested by Lee and Albaisa [19] who performed stress controlled tests on Monterey sand specimens. However, peak pore pressures were consistent with lower and upper boundaries suggested by Dash and Sitharam [15] who performed stress controlled tests on Ahmedabad sand and Quarry dust as silt. This type of observation was observed for all the specimens with any silt content in this test program corresponding to any approach due to the presence of fines.

To determine the cyclic shear strength or cyclic resistance ratio (CRR) of a specimen of desired silt content and relative density corresponding to the concerned approach, a minimum of three cyclic tests were carried out at different cyclic stress ratios (CSR) till the initial liquefaction (excess pore water pressure) became equal to the initial consolidation stress, $\sigma'_{3c}$ or ±3% axial strain was reached as discussed earlier. Thereafter these cyclic stress ratios were plotted against the corresponding cycles to initial liquefaction ($N_L$) as shown in Fig. 7 for a specimen with 80% silt content at post consolidation relative densities of 60%. CRR was determined as the CSR corresponding to liquefaction at 15 cycles.

### 3.2. Constant dry density approach

Fig. 8 illustrates the liquefaction susceptibility of sand–silt mixtures with varying percentages of non-plastic fines at a constant dry density of 13.6 kN/m$^3$ and CSR=0.10. As seen, the liquefaction potential is influenced by the non-plastic fines. This clearly indicates that the percentage of non-plastic fines in the sand samples has a significant effect on the liquefaction potential. It is seen that the liquefaction potential of the sand sample increases with increase of non-plastic fines up to 30% (till limiting silt content). However, with further increase in non-plastic fines (FC > 30%) the liquefaction potential is found to be decreasing. This may be attributed to the change in the sand matrix from sand controlled matrix to silt controlled matrix. This result is in very good agreement with the experimental investigation of Dash and Sitharam [15]; Sitharam et al. [24]. The experimental results from the current study indicate that the threshold value (limiting value) of fines content is approximately equal to 30% which is equal to the limiting fines content value calculated using Eq. (1) [19].

### 3.3. Constant relative density approach

Initially the number of cycles required generating 100% excess pore water pressure or ±3% axial strain in the specimens at a constant cyclic stress ratio of 0.10 was studied and is presented in Fig. 9. It is observed from this figure that the cycles of loading decreased till around the limiting silt content and beyond this point it remains more or less same with further increase in silt content till even pure silt. This observation indicates that in constant relative density approach the cyclic resistance decreases rapidly till around the limiting silt content and beyond limiting silt content it remains relatively same for all the silt contents till pure silt.

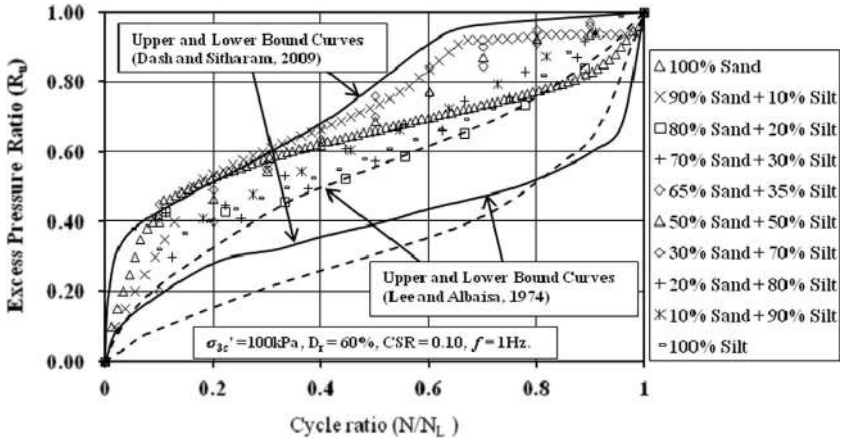


**Fig. 6.** Typical pore pressure response against cycle ratio as per the method suggested by Lee and Albaisa [19]; Dash and Sitharam [15].

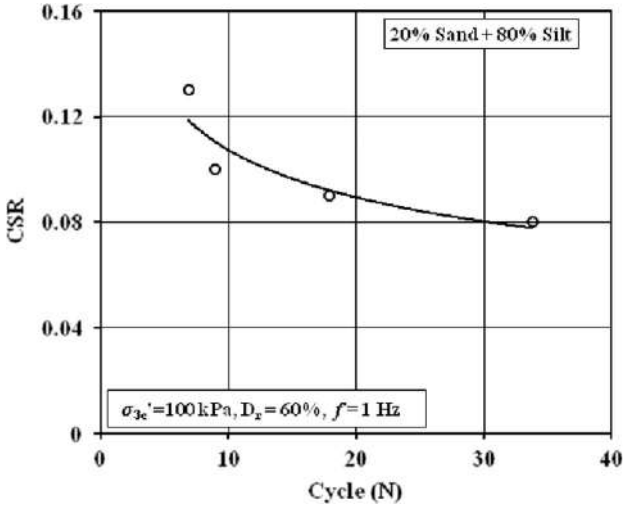


**Fig. 7.** Typical cyclic stress ratio curve.

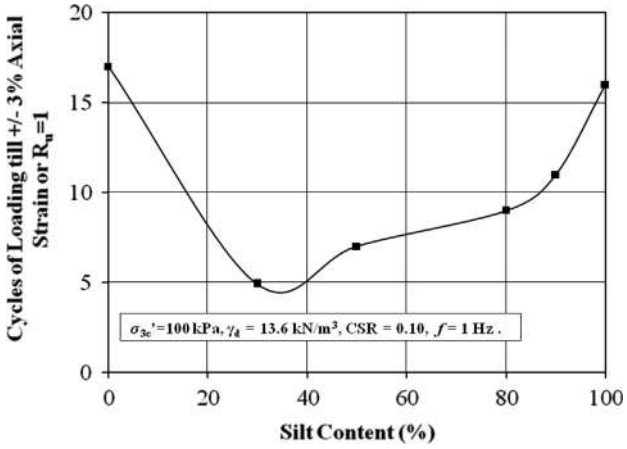


**Fig. 8.** Cycles of loading till initial liquefaction with different percentages of non-plastic silt at CSR=0.10 and constant dry density=13.6 kN/m$^3$.

The peak pore pressure response as a function of cycles of loading is presented in Fig. 10 where it was seen that the rate of generation of excess pore water pressure decreases rapidly till around the limiting silt content and finally it remains relatively same for all the silt contents till even pure silt, thus justifying the cyclic resistance behavior as described above. Fig. 11 shows the variation of dry density of sand–silt mixture with silt content at a

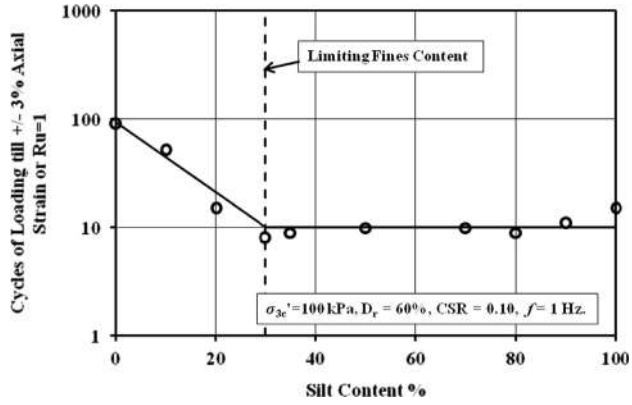


**Fig. 9.** Cycles of loading till $R_u=1$ or $\pm 3\%$ axial strain versus silt content at $D_r=60\%$ and CSR=0.10.

constant relative density of 60%. After limiting silt content dry density decreases with increase of silt content. Therefore the variation of cyclic resistance with silt content cannot be attributed to dry density. The effect of fines in reducing the cyclic resistance despite an increase in dry density till the limiting silt content was found in line with Dash and Sitharam [15]. But it should be noted that Dash and Sitharam [15] prepared the sample by the dry deposition method, whereas moist tamping method was used in this study. A comparison between materials used in this study and Dash and Sitharam [15] is given in Table 4.

Also the effect of fines can well be understood in keeping the cyclic resistance relatively same despite a decrease in dry density with increase in silt content beyond the limiting silt content because the presence of more fines in a specimen at a constant relative density resists the development of excess pore water pressure and this prevents the likely fall in cyclic resistance.

### 3.4. Effect of non-plastic silt on pore pressure generation

The data collected during the series of cyclic stress control triaxial tests to study the liquefaction potential of clean sand, silt and sand–silt mixtures with varying non-plastic silt content were used to understand in detail the development of excess pore water pressure in the sand samples. The effects of amplitude of cyclic shear strain, relative density, confining pressure, percentage of non-plastic fines and the number of loading cycles are presented here. Fig. 12 illustrates the relationship between the pore pressure ratio and number of loading cycles for 20% sand and 80% silt at different CSR values subjected to initial liquefaction. It is evident from Fig. 12 that the development of pore pressure ratio is a

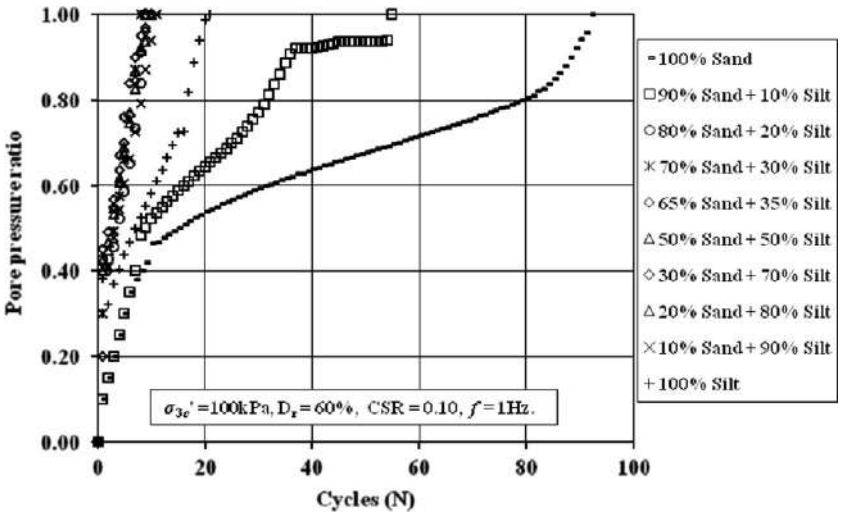


**Fig. 10.** Pore pressure response as a function of cycles of loading at $D_r = 60\%$.

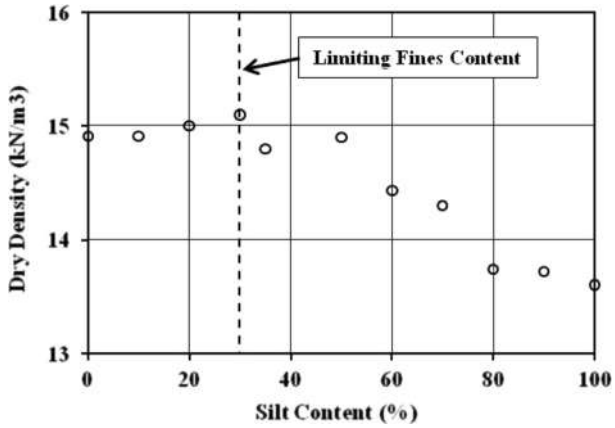


**Fig. 11.** Variation of dry density with silt content at $D_r = 60\%$.

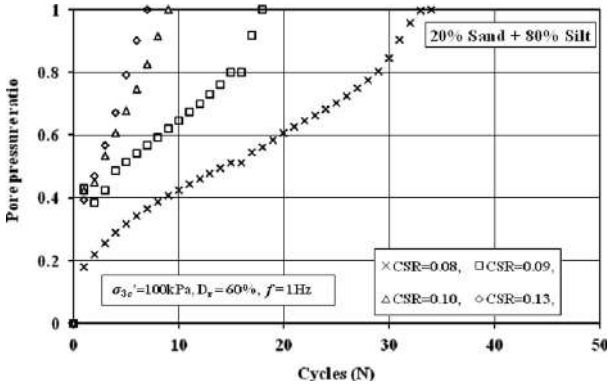


**Fig. 12.** Relationship between pore water pressure ratio and number of cycle for 80% silt, $D_r = 60\%$ at various cyclic stress ratios.

**Table 4**
Comparison between materials used in this study and Dash and Sitharam [15].

| Properties | | **Studied sample** | **Studied sample by Dash and Sitharam [15]** |
|---|---|---|---|
| Source of non-plastic silt | | Natural deposit | Rubble crush |
| Mean grain size $D_{50}$ | Sand | 0.203 | 0.375 |
| | Silt | 0.022 | 0.037 |
| Method of sampling | | Moist tamping | Dry deposit |
| Relative density (studied) | | 60 (%) | 53 (%) |
| Specimen size | | Dia. 50 mm and height 100 mm | Dia. 71 mm and height 142 mm |

function of CSR and number of cycles. Pore pressure ratio increases with increase in CSR. For a low amplitude of CSR (0.08), the pore pressure ratio develops gradually with the number of cycles and for higher CSR (0.13) the pore pressure ratio develops suddenly within a few cycles.

Fig. 13 illustrates the effect of relative density on pore pressure generation with number of loading cycles at CSR 0.10. It is clearly seen from this Figure that as the relative density increases there is a decrease in the rate of buildup of pore pressure, which signifies the influence of relative density on the generation of pore water pressure. Dash and Sitharam [15] also reported similar behavior on Ahemedabad sand Quarry dust (silt) from stress controlled cyclic tests results.

Fig. 14 shows the effect of non-plastic silt content on the pore pressure generation with number of loading cycles for a constant dry density of 13.6 kN/m$^3$ at 1 Hz frequency under an effective confining pressure of 100 kPa. It has been observed that pore pressure ratio increases with increase in percentage of non-plastic fines (FC < 30%). With further increase in non-plastic fines (FC > 30%) excess pore pressure ratio decreased. In addition, number of cycles for initial liquefaction decreases with increase in the percentage of non-plastic fines content (FC < 30%). However, with further increase in the non-plastic fines (FC > 30%) the number of cycles for initial liquefaction has been found to increase. This clearly indicates that for non-plastic fine content greater than 30%, there is a change in the matrix of the sand from sand controlled matrix to silt controlled matrix. As fine content dominates it prevents the building up of pore pressure, thus influencing the potential for liquefaction.

### 3.5. *Effect of non-plastic silt on permeability*

According to the definition of limiting fines content after LFC the soil specimens behave as silt, for experimental evidence, permeability test by falling head method on sand–silt mixtures was performed at a $D_r = 60\%$. Fig. 15 shows the variation of permeability

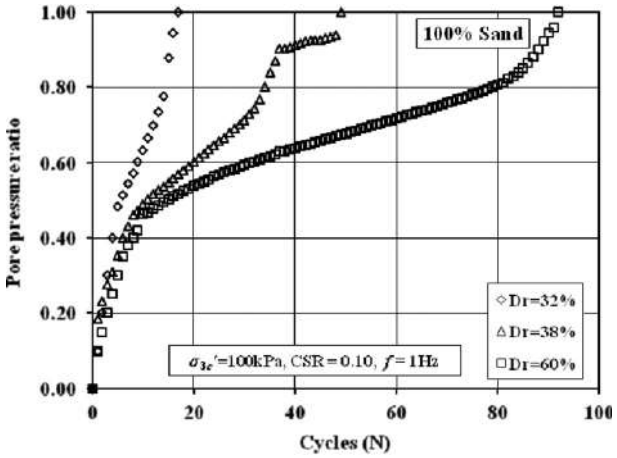


**Fig. 13.** Effect of relative density on the pore pressure generation with number of loading cycles for clean sand at CSR=0.10.

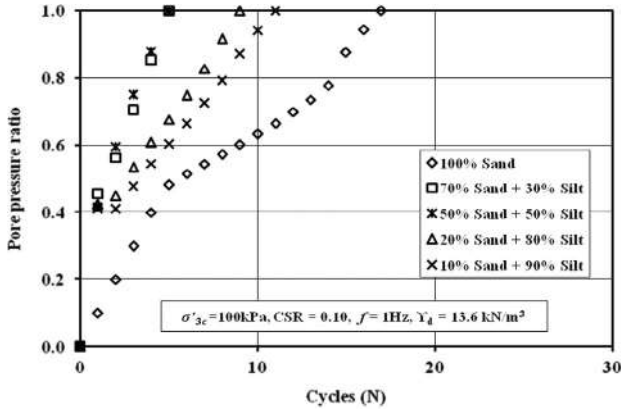


**Fig. 14.** Variation of pore pressure ratio with numbers of cycles for different percentages of non-plastic fines.

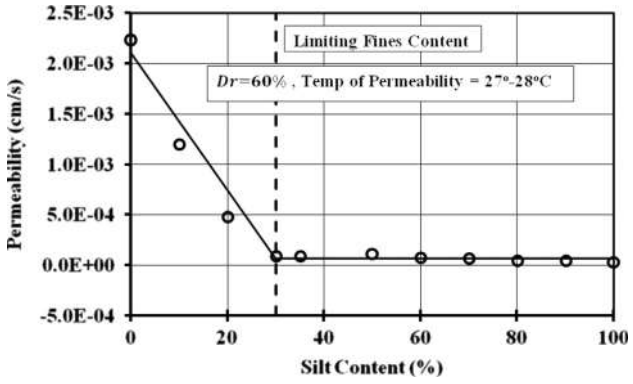


**Fig. 15.** Variation of permeability with silt content.

with silt content. For increasing silt content the permeability decreases till LFC; after LFC the permeability becomes constant with silt content. That means the concept of limiting silt content worked well in permeability. This is the reason why liquefaction resistance decreases with the increase of silt content up to LFC and remains constant thereafter (as in Fig. 9). After LFC permeability remains constant at the same relative density which proves that after LFC the inner void of fine particles remains almost same.

### 3.6. Effect of non-plastic silt on cyclic resistance ratio

Cyclic resistance Ratio (CRR) of sand–silt mixture of desired silt content and relative density 60% was determined as CSR at which liquefaction occurred for 15 cycles of loading. Fig. 16 shows the variation of CRR with silt content. Up to LFC, CRR decreased; after that CRR remained constant. Concept of LFC worked for CRR well.

### 3.7. Effect of non-plastic silt on shear modulus

Secant shear modulus was determined at the 2nd cycle. The target was to determine secant shear modulus at the 2nd cycle for all specimens so that it can be compared. Fig. 17 shows the secant shear modulus variation with silt content. It was observed that with increasing silt content the secant shear modulus ($G_{sec}$) decreases till LFC=30%; after LFC $G_{sec}$ became constant. Examining the data it was found that shear strain ranges from 0.0009 to 0.0033 as shown in Fig. 17. So, the change of secant shear modulus was due to strain level change.

### 3.8. Combined pore pressure analysis

Lee and Albaisa [19] carried out around 22 cyclic triaxial tests with varying parameters on Monterey river sand to study the pore pressure response of sand. They varied the relative density from around 30% to 100%, confining pressure from 103 kPa to 1378 kPa and cyclic stress ratio from 0.24 to 0.38. They reported that all the curves generated by plotting the pore pressure response against the corresponding cycle ratio fall within a relatively narrow band. Results obtained from this investigation were utilized to study the limitations of this band when non-plastic fines are added to sand. For this purpose, peak pore pressures generated in sand–silt mixture specimens prepared at various relative densities corresponding to all the approaches over a wide range of parameters are presented as a function of cycle ratio ($N/N_L$) in Fig. 18 to assess the upper and lower bound values as suggested by Lee and Albaisa [19]. Dash and Sitharam [15] carried out around 289 cyclic triaxial

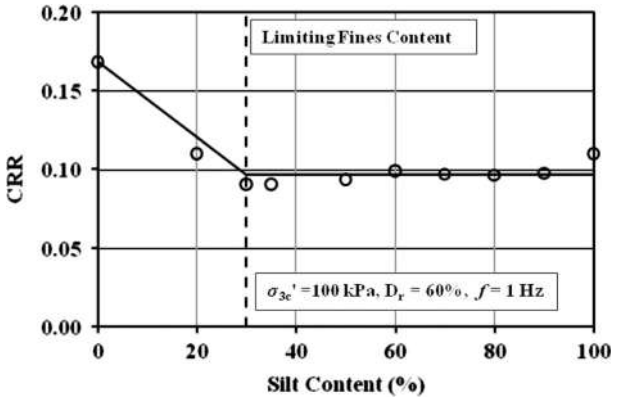


**Fig. 16.** Variation of cyclic resistant ratio (CRR) with silt content.

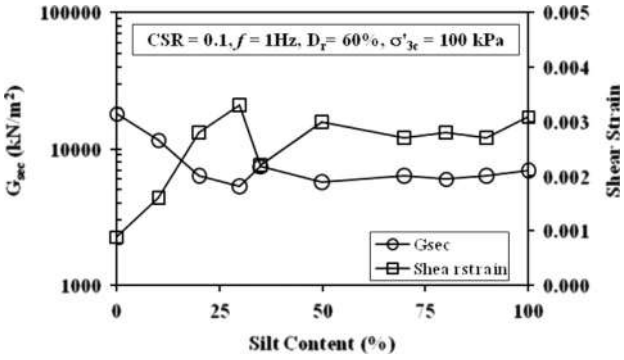


**Fig. 17.** Variation of secant shear modulus at 2nd cycle with silt content.

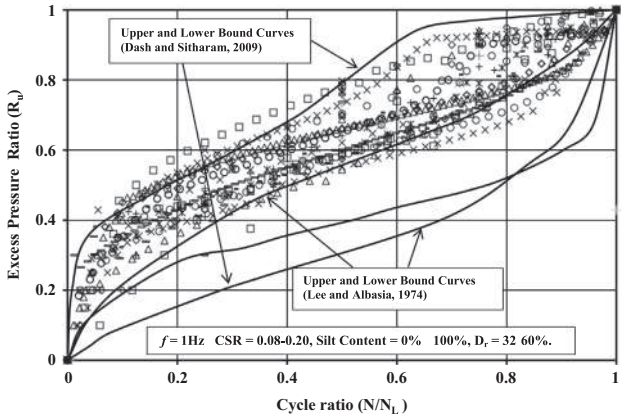


**Fig. 18.** Maximum and minimum peak pore generation in sand and silt mixture specimens over a wide range of parameters and compared with Lee and Albasia [19]; Dash and Sitharam [15].

tests with varying parameters on Ahmedabad sand to study the pore pressure response of sand. They varied the relative density from around 14 to 91%, confining the pressure from 50 kPa to 200 kPa and cyclic stress ratio from 0.092 to 0.205 and proposed a new pore pressure band for sand–silt mixtures in line with Lee and Albaisa [19].

A check of pore pressure band for sand–silt mixtures has been presented in Fig. 18. The peak pore pressures generated in sand–silt mixture specimens prepared at a relative density of 60%, confining pressure of 100 kPa and cyclic stress ratio from 0.08 to 0.20 are presented in Fig. 18. The pore pressure band proposed by Dash and Sitharam [15] was found to be valid for sand–silt mixtures used in this study.

## 4. Conclusion

The rate of generation of excess pore water pressure with respect to cycles of loading was found to initially increase with increase in silt content till the limiting silt content (LFC) is reached and thereafter it reverses its trend when the specimens were tested at a constant dry density. This behavior was found to be due to corresponding initial decrease and then increase in relative density of the specimens. The cyclic resistance behavior was observed to be just opposite to the pore pressure response. In constant relative density approach, the excess pore pressure generation rate with respect to cycles of loading was found to initially decrease till limiting silt content and thereafter a more or less same rate till even pure silt. This pore pressure response implies that the cyclic resistance decreases till the limiting silt content and thereafter remains relatively constant. Permeability, CRR and secant shear modulus decreased till limiting silt content; after that they became constant with increasing silt content.

## Acknowledgments

The authors express their sincere gratitude for the financial assistance and laboratory facilities received from Bangladesh University of Engineering and Technology.

## References

[1] Kishida H. Characteristics of liquefied sands during Mino-Owari,Tohnankai, and Fukui earthquakes. Soils Found 1969;9(1):75–92.
[2] Tohno I, Yasuda S. Liquefaction of the ground during the 1978 Miyagiken-Oki earthquake. Soils Found 1981;21(3):18–34.
[3] Seed HB, Tokimatsu K, Harder LF, Chung RM. The influence of SPT procedures in soil liquefaction resistance evaluations. J Geotech Eng 1985;111(12):1425–45.
[4] Chang NY, Yeh ST, Kaufman LP. Liquefaction potential of clean and siltysands. In: Proceedings of 3rd international conference on earthquake microzonation, vol. 2; 1982. p. 1017–32.
[5] Amini F, Qi GZ. Liquefaction testing of stratified silty sands. J Geotech Geoenviron Eng 2000;126(3):208–17.
[6] Kuerbis RH, Negussey D, Vaid YP. Effect of gradation and fines content on the undrainedresponse of sand. In: Proceedings on hydraulic fill structures, Geotechnical Special Publication, ASCE, vol. 21; 1988. p. 330–45.
[7] Finn WDL, Ledbetter RH, Wu G. Liquefaction in silty soils: design and analysis. Ground failures under seismic conditions, 44. USA: Geotechnical Special Publication, ASCE; 1994; 51–74.
[8] Polito CP, Martin II JR. Effects of nonplastic fines on the liquefaction resistance of sands. J Geotech Geoenviron Eng 2001;127(5):408–15.
[9] Koester JP. The influence of fine type and content on cyclic strength: ground failures under seismic conditions. Geotechnical Special Publication, 44. USA: ASCE; 1994. p. 330–45.
[10] Xenaki VC, Athanasopoulos GA. Liquefaction resistance of sand–silt mixtures: an experimental investigation of the effect of fines. Soil Dyn Earthq Eng 2003;23:183–94.
[11] Ueng TS, Sun CW, Chen CW. Definition of fines and liquefaction resistance of Maoluo river soil. Soil Dyn Earthq Eng 2004;24:745–75.
[12] Ravishankar BV. Cyclic and monotonic undrained behavior of sandy soils [Ph.D. thesis]. Indian Institute of Science, Bangalore in the Faculty of Engineering; 2006.
[13] KenanandandM. H, Ellen R. Pore pressure generation of silty sands due to induced cyclic shear strains. J Geotech Geoenviron Eng, ASCE. 2009; 1892–905 (December).
[14] Singh S. Liquefaction characteristics of silts. Ground failure under seismic conditions, 44. Geotechnical Special Publication, ASCE; 1994; 105–16.
[15] Dash HK, Sitharam TG. Undrained cyclic pore pressure response of sand–silt mixtures: effect of nonplastic fines and other parameters. Geotech Geol Eng 2009;27:501–17.
[16] Shen CK, Vrymoed JL, Uyeno CK. The effects of fines on liquefaction of sands. In: Proceedings of the 9th international conference on soil mechanics and foundation engineering, vol. 2; 1977. p. 381–5.
[17] Kuerbis R, Negussey D, Vaid YP. Effect of gradation and fines content on the undrained response of sand. In: Proceedings on hydraulic fill structures, Geotechnical Special Publication. ASCE, vol. 21; 1988. p. 330–45.
[18] Vaid YP. Liquefaction of silty soils. Ground failure under seismic conditions, 44. Geotechnical Special Publication. ASCE; 1994; 1–16.
[19] Lee KL, Albaisa A. Earthquake induced settlements in saturated sands. J Geotech Eng Div 1974;100(GT4):387–406.
[20] Polito CP. The effect of nonplastic and plastic fines on the liquefaction of sandy soils [Ph.D. thesis], Blacksdurg: Verginia Polytechnic Institute and State University, va. (this document may be accessed at ⟨http://scholar.lib.vt.edu/theses/available/etd-122299-125729⟩).
[21] Head KH. Manual of soil laboratory testing, volume 1: soil classification tests. Scotland, UK: ELE International Limited; 1984; 139–40.
[22] Hazirbaba K. Pore pressure generation characteristics of sand and silty sands: a strain approach. 2005 (Dissertation presented for Ph.D. program to the faculty of Graduate School, University of Texas).
[23] Ladd RS. Preparing test specimens using under compaction. Geotech Test J 1978;1(1):16–23.
[24] Sitharam TG, Ravishankar BV, Vinod JS. Liquefaction and pore water pressure generation in sand—a cyclic strain approach. J Earthq Tsunami 2008;2 (3):227–40.